PROCEEDINGS OF SCIENCE

2019 Update on ε_K with lattice QCD inputs

Jeehun Kim, Sunkyu Lee, Weonjong Lee[*]
Lattice Gauge Theory Research Center, CTP, and FPRD,
Department of Physics and Astronomy,
Seoul National University, Seoul 08826, South Korea
E-mail: wlee@snu.ac.kr

Yong-Chull Jang
Physics Department, Brookhaven National Laboratory, Upton, NY11973, USA

Jaehoon Leem
School of Physics, Korea Institute for Advanced Study (KIAS), Seoul 02455, South Korea

Sungwoo Park
Los Alamos National Laboratory, Theoretical Division T-2, Los Alamos, NM87545, USA

LANL-SWME Collaboration

We present updated results for ε_K determined directly from the standard model (SM) with lattice QCD inputs such as $\hat{B}_K$, $|V_{cb}|$, $|V_{us}|$, ξ_0, ξ_2, ξ_{LD}, f_K, and m_c. We find that the standard model with exclusive $|V_{cb}|$ and other lattice QCD inputs describes only 65% of the experimental value of $|\varepsilon_K|$ and does not explain its remaining 35%, which leads to a strong tension in $|\varepsilon_K|$ at the $4.6\sigma \sim 4.2\sigma$ level between the SM theory and experiment. We also find that this tension disappears when we use the inclusive value of $|V_{cb}|$ obtained using the heavy quark expansion based on QCD sum rules.

37th International Symposium on Lattice Field Theory - Lattice2019
16-22 June 2019
Wuhan, China

[*]Speaker.

PoS(LATTICE2019)029

1. Introduction

This paper is an update of our previous papers [1, 2, 3, 4, 5]. Here, we present recent progress in determination of $|\varepsilon_K|$ with updated inputs from lattice QCD.

2. Input parameters: $|V_{cb}|$

In Table 1 (a) and (d), we present updated results for exclusive $|V_{cb}|$ and inclusive $|V_{cb}|$ respectively. In Table 1 (a), we present results for exclusive $|V_{cb}|$ of BELLE [6] and BABAR [7]. They reported results obtained using both CLN and BGL methods, which turn out to be consistent with each other.

In Table. 1 (c), we plot time evolution of the $|V_{cb}|$ results for the CLN analysis (blue line) as well as the BGL analysis (red line) for the $\bar{B} \to D^* \ell \bar{\nu}$ decays. Here, the black cross symbols with label Gambino represent results from Refs. [8, 9, 10], respectively. The brown square symbol with label Grinstein represents results from Ref. [11]. The green circle symbol with label BELLE-17 represents results from Ref. [12]. The magenta circle symbols with label BELLE-18 represent results from Ref. [6]. The green triangle symbols with label BELLE-19 represent results from Ref. [13]. The orange diamond symbols with label BABAR represents results from Ref. [7]. In 2017 when Bigi, Gambino, and Schacht [8, 11] first raised a claim that there might be an inconsistency in exclusive $|V_{cb}|$ between the CLN and BGL analyses on the BELLE-2017 tagged data set of the $\bar{B} \to D^* \ell \bar{\nu}$ decays, the BGL results seemed to be superficially consistent with those for inclusive $|V_{cb}|$. However, the 2019 analyses of both BELLE [6] (on the untagged data) and BABAR [7] show that the results of the BGL analysis might be consistent with those of the CLN analysis, which denies the previous claim of Refs. [8, 11]. The pink dashed line with label FLAG-19 represents preliminary results of BELLE-18 which the FLAG 2019 report took over to do their analysis on $|V_{cb}|$. Hence, if you are to use the $|V_{cb}|$ results of FLAG 2019, please do it with proper caution, since they might be out of date. The green dashed line with label SWME-19 represents results of BELLE-19 [6] which we use for the analysis on ε_K in this paper.

In Table 1 (b), we show the plot made by HFLAV. Results on this plot are available on the web [14], but not published in any journal yet. Recently, there has been an interesting claim that the $|V_{cb}|$ puzzle might be resolved if we include $\mathcal{O}(1/m_c^2)$ corrections in the data analysis [15].

3. Input parameter ξ_0

The absorptive part of long distance effects on ε_K is parametrized into ξ_0.

$$\xi_0 = \frac{\text{Im}A_0}{\text{Re}A_0}, \qquad \xi_2 = \frac{\text{Im}A_2}{\text{Re}A_2}, \qquad \text{Re}\left(\frac{\varepsilon'}{\varepsilon}\right) = \frac{\omega}{\sqrt{2}|\varepsilon_K|}(\xi_2 - \xi_0)\,. \tag{3.1}$$

There are two independent methods to determine ξ_0 in lattice QCD: the indirect and direct methods. The indirect method is to determine ξ_0 using Eq. (3.1) with lattice QCD results for ξ_2 combined with experimental results for ε'/ε, ε_K, and ω. The direct method is to determine ξ_0 directly using the lattice QCD results for ImA_0, combined with experimental results for ReA_0. In Table 1 (e), we summarize results for ξ_0 calculated by RBC-UKQCD. Here, we use the results of the indirect method for ξ_0 to evaluate ε_K, since its systematic and statistical errors are much smaller.

PoS(LATTICE2019)029

channel	method	value	Ref.
combined		39.13(59)	HFLAV-17 [16]
combined		39.25(56)	HFLAV-19 [14]
$\bar{B} \to D^* \ell \bar{\nu}$	CLN	38.4(2)(6)(6)	BELLE-19 [6]
$\bar{B} \to D^* \ell \bar{\nu}$	BGL	38.3(3)(7)(6)	BELLE-19 [6]
$\bar{B} \to D^* \ell \bar{\nu}$	CLN	38.40(84)	BABAR-19 [7]
$\bar{B} \to D^* \ell \bar{\nu}$	BGL	38.36(90)	BABAR-19 [7]

(a) Exclusive $|V_{cb}|$ in units of 10^{-3}.

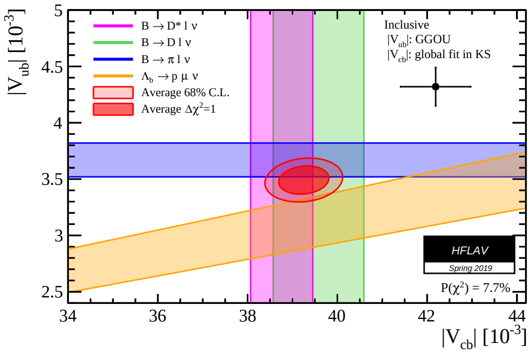

(b) $|V_{cb}|$ versus $|V_{ub}|$.

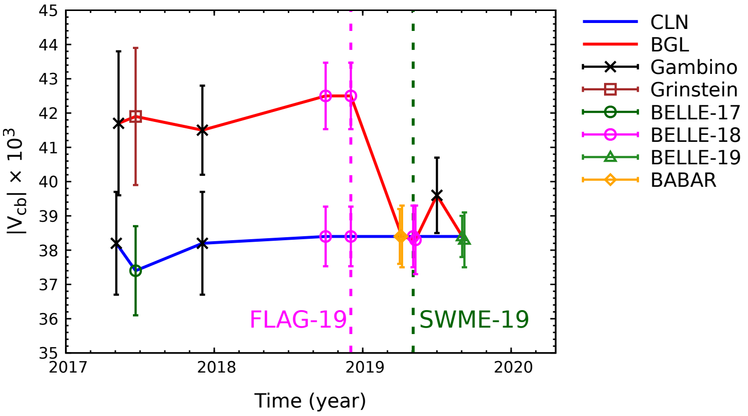

(c) CLN versus BGL.

channel	value	Ref.
kinetic scheme	42.19(78)	[16]
1S scheme	41.98(45)	[16]

(d) Inclusive $|V_{cb}|$ in units of 10^{-3}.

method	ξ_0	Ref.
indirect	$-1.63(19) \times 10^{-4}$	[17]
direct	$-0.57(49) \times 10^{-4}$	[18]

(e) Results for ξ_0.

Table 1: Results for $|V_{cb}|$: (a) exclusive $|V_{cb}|$, (b) $|V_{cb}|$ versus $|V_{ub}|$, (c) Time evolution for exclusive $|V_{cb}|$ obtained using CLN and BGL, and (d) inclusive $|V_{cb}|$; (e) results for ξ_0.

4. Input parameters: Wolfenstein parameters, $\hat{B}_K$, $\xi_{\rm LD}$, and others

WP	CKMfitter		UTfit		AOF	
λ	0.22475(25)	[19]	0.22500(100)	[20]	0.2243(5)	[21]
$\bar{\rho}$	0.1577(96)	[19]	0.148(13)	[20]	0.146(22)	[22]
$\bar{\eta}$	0.3493(95)	[19]	0.348(10)	[20]	0.333(16)	[22]

(a) Wolfenstein parameters

Input	Value	Ref.
η_{cc}	1.72(27)	[2]
η_{tt}	0.5765(65)	[23]
η_{ct}	0.496(47)	[24]

(b) η_{ij}

Table 2: (a) Wolfenstein parameters and (b) QCD corrections: η_{ij} with $i, j = c, t$.

In Table 2 (a), we present the Wolfenstein parameters on the market. As explained in Ref. [1, 5], we use the results of angle-only-fit (AOF) in Table 2 (a) in order to avoid unwanted correlation between $(\varepsilon_K, |V_{cb}|)$, and $(\bar{\rho}, \bar{\eta})$. We determine λ from $|V_{us}|$ which is obtained from the $K_{\ell 2}$ and $K_{\ell 3}$ decays using lattice QCD inputs for form factors and decay constants. We determine the A parameter from $|V_{cb}|$.

In FLAG 2019 [25], they report lattice QCD results for $\hat{B}_K$ with $N_f = 2$, $N_f = 2+1$, and $N_f = 2+1+1$. Here, we use the results for $\hat{B}_K$ with $N_f = 2+1$, which is obtained by taking an average over the four data points from BMW 11, Laiho 11 RBC-UKQCD 14, and SWME 15 in Table 3 (a).

Collaboration	Ref.	$\hat{B}_K$
SWME 15	[26]	0.735(5)(36)
RBC/UKQCD 14	[27]	0.7499(24)(150)
Laiho 11	[28]	0.7628(38)(205)
BMW 11	[29]	0.7727(81)(84)
FLAG 2019	[25]	0.7625(97)

(a) $\hat{B}_K$

Input	Value	Ref.
G_F	$1.1663787(6)\times 10^{-5}$ GeV^{-2}	PDG-19 [21]
M_W	80.379(12) GeV	PDG-19 [21]
θ	$43.52(5)^\circ$	PDG-19 [21]
m_{K^0}	497.611(13) MeV	PDG-19 [21]
ΔM_K	$3.484(6)\times 10^{-12}$ MeV	PDG-19 [21]
F_K	155.7(3) MeV	FLAG-19 [25]

(b) Other parameters

Table 3: (a) Results for $\hat{B}_K$ and (b) other input parameters.

Collaboration	N_f	$m_c(m_c)$	Ref.
FLAG 2019	$2+1$	1.275(5)	[25]
FLAG 2019	$2+1+1$	1.280(13)	[25]

(a) $m_c(m_c)$ [GeV]

Collaboration	M_t	$m_t(m_t)$	Ref.
PDG 2018	173.0 ± 0.4	$163.17\pm0.38\pm0.17$	[21]
PDG 2019	172.9 ± 0.4	$163.08\pm0.38\pm0.17$	[21]

(b) $m_t(m_t)$ [GeV]

Table 4: Results for (a) charm quark mass and (b) top quark mass.

The dispersive long distance (LD) effect is defined as

$$\xi_{\rm LD} = \frac{m'_{\rm LD}}{\sqrt{2}\Delta M_K}, \qquad m'_{\rm LD} = -\text{Im}\left[\mathscr{P}\sum_C \frac{\langle \overline{K}^0|H_{\rm w}|C\rangle\langle C|H_{\rm w}|K^0\rangle}{m_{K^0}-E_C}\right] \tag{4.1}$$

As explained in Refs. [1], there are two independent methods to estimate $\xi_{\rm LD}$: one is the BGI estimate [30], and the other is the RBC-UKQCD estimate [31, 32]. The BGI method is to estimate the size of $\xi_{\rm LD}$ using chiral perturbation theory as follows,

$$\xi_{\rm LD} = -0.4(3)\times\frac{\xi_0}{\sqrt{2}} \tag{4.2}$$

The RBC-UKQCD method is to estimate the size of $\xi_{\rm LD}$ as follows,

$$\xi_{\rm LD} = (0\pm 1.6)\%. \tag{4.3}$$

Here, we use both methods to estimate the size of $\xi_{\rm LD}$.

In Table 2 (b), we present higher order QCD corrections: η_{ij} with $i,j=t,c$. A new approach using $u-t$ unitarity instead of $c-t$ unitarity appeared in Ref. [33], which is supposed to have a better convergence with respect to the charm quark mass. Here, we have not incorporated this into our analysis yet, but will do it in near future.

In Table 3 (b), we present other input parameters needed to evaluate ε_K. Here, the W boson mass M_W and the kaon decay constant F_K have been updated since Lattice 2018. In Table 4, we present the charm quark mass $m_c(m_c)$ and top quark mass $m_t(m_t)$. From FLAG 2019 [25], we take the results for $m_c(m_c)$ with $N_f=2+1$, since there is some discrepancy in those with $N_f=2+1+1$. For the top quark mass, we use the PDG 2019 results to obtain $m_t(m_t)$.

5. Results for ε_K

In Fig. 1, we show results for $|\varepsilon_K|$ evaluated directly from the standard model (SM) with lattice QCD inputs given in the previous sections. In Fig. 1 (a), the blue curve represents the theoretical

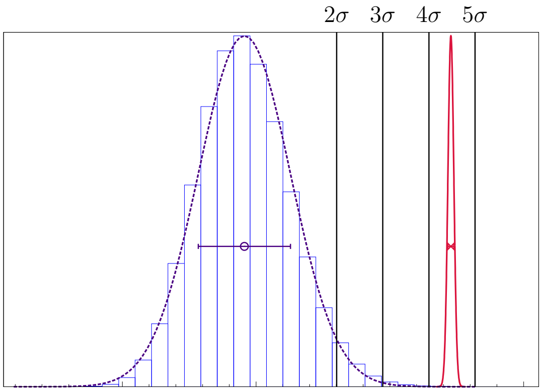

(a) Exclusive $|V_{cb}|$ (BELLE-19, CLN)

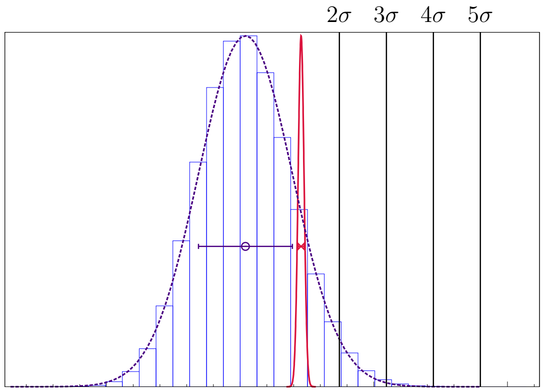

(b) Inclusive $|V_{cb}|$ (1S scheme)

Figure 1: $|\varepsilon_K|$ with (a) exclusive $|V_{cb}|$ (left) and (b) inclusive $|V_{cb}|$ (right) in units of 1.0×10^{-3}.

evaluation of $|\varepsilon_K|$ obtained using the FLAG-2019 results for $\hat{B}_K$, AOF for Wolfenstein parameters, the (BELLE-19, CLN) results for exclusive $|V_{cb}|$, and the RBC-UKQCD estimate for ξ_{LD}. The red curve in Fig. 1 represents the experimental results for $|\varepsilon_K|$. In Fig. 1 (b), the blue curve represents the same as in Fig. 1 (a) except for using the 1S scheme results for the inclusive $|V_{cb}|$.

Our results for $|\varepsilon_K|^{\text{SM}}$ are summarized in Table 5. Here, the superscript $^{\text{SM}}$ represents the theoretical expectation value of $|\varepsilon_K|$ obtained directly from the SM. The superscript $^{\text{Exp}}$ represents the experimental value of $|\varepsilon_K| = 2.228(11) \times 10^{-3}$. Results in Table 5 (a) are obtained using the RBC-UKQCD estimate for ξ_{LD}, and those in Table 5 (b) are obtained using the BGI estimate for ξ_{LD}. In Table 5 (a), we find that the theoretical expectation values of $|\varepsilon_K|^{\text{SM}}$ with lattice QCD inputs (with exclusive $|V_{cb}|$) has $4.6\sigma \sim 4.2\sigma$ tension with the experimental value of $|\varepsilon_K|^{\text{Exp}}$, while there is no tension with inclusive $|V_{cb}|$ (obtained using heavy quark expansion and QCD sum rules).

$\lvert V_{cb}\rvert$	method	reference	$\lvert\varepsilon_K\rvert^{\text{SM}}$	$\Delta\varepsilon_K$
exclusive	CLN	BELLE-19	1.456 ± 0.172	4.47σ
exclusive	BGL	BELLE-19	1.443 ± 0.181	4.32σ
exclusive	CLN	BABAR-19	1.456 ± 0.169	4.55σ
exclusive	BGL	BABAR-19	1.451 ± 0.175	4.44σ
exclusive	combined	HFLAV-19	1.576 ± 0.154	4.23σ
inclusive	kinetic	HFLAV-17	2.060 ± 0.212	0.79σ
inclusive	1S	HFLAV-17	2.020 ± 0.176	1.18σ

(a) RBC-UKQCD estimate for ξ_{LD}

$\lvert V_{cb}\rvert$	method	reference	$\lvert\varepsilon_K\rvert^{\text{SM}}$	$\Delta\varepsilon_K$
exclusive	CLN	BELLE-19	1.501 ± 0.174	4.16σ
exclusive	BGL	BELLE-19	1.488 ± 0.183	4.04σ

(b) BGI estimate for ξ_{LD}

Table 5: $|\varepsilon_K|$ in units of 1.0×10^{-3}, and $\Delta\varepsilon_K = |\varepsilon_K|^{\text{Exp}} - |\varepsilon_K|^{\text{SM}}$.

In Fig. 2 (a), we show the time evolution of $\Delta\varepsilon_K$ starting from 2012 to 2019. In 2012, $\Delta\varepsilon_K$ was 2.5σ, but now it is 4.5σ with exclusive $|V_{cb}|$ (BELLE-19, CLN). In Fig. 2 (b), we show the time evolution of the average $\Delta\varepsilon_K$ and the error $\sigma_{\Delta\varepsilon_K}$ during the period of 2012–2019.

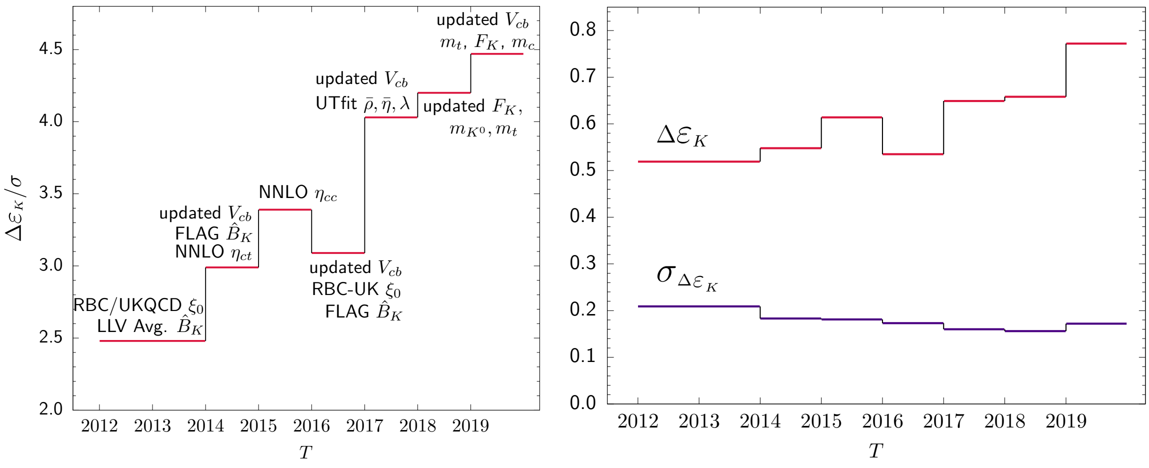

(a) Time evolution of $\Delta\varepsilon_K/\sigma$

(b) Time evolution of the average and error of $\Delta\varepsilon_K$

Figure 2: Time history of (a) $\Delta\varepsilon_K/\sigma$, and (b) $\Delta\varepsilon_K$ and $\sigma_{\Delta\varepsilon_K}$.

At present, we find that the largest error ($\approx 50\%$) in $|\varepsilon_K|^{\text{SM}}$ comes from $|V_{cb}|$. Hence, it is of crucial importance to reduce the error in $|V_{cb}|$ significantly. To achieve this goal, there is an on-going project to extract exclusive $|V_{cb}|$ using the Oktay-Kronfeld (OK) action for the heavy quarks to calculate the form factors for $\bar{B} \to D^{(*)}\ell\bar{\nu}$ decays [34, 35, 36, 37, 38].

Acknowledgments

We thank Rajan Gupta, Andrew Lytle, and Martin Jung for helpful discussion. The research of W. Lee is supported by the Mid-Career Research Program (Grant No. NRF-2019R1A2C2085685) of the NRF grant funded by the Korean government (MOE). This work was supported by Seoul National University Research Grant in 2019. W. Lee would like to acknowledge the support from the KISTI supercomputing center through the strategic support program for the supercomputing application research (No. KSC-2017-G2-0009). Computations were carried out on the DAVID cluster at Seoul National University.

References

[1] J. A. Bailey *et al.* *Phys. Rev.* **D98** (2018), no. 9 094505, [1808.09657].

[2] J. A. Bailey, Y.-C. Jang, W. Lee, and S. Park *Phys. Rev.* **D92** (2015), no. 3 034510, [1503.05388].

[3] J. A. Bailey *et al.* *PoS* **LATTICE2018** (2018) 284, [1810.09761].

[4] Y.-C. Jang, W. Lee, S. Lee, and J. Leem *EPJ Web Conf.* **175** (2018) 14015, [1710.06614].

[5] J. A. Bailey, Y.-C. Jang, W. Lee, and S. Park *PoS* **LATTICE2015** (2015) 348, [1511.00969].

[6] **Belle** Collaboration, E. Waheed *et al.* *Phys. Rev.* **D100** (2019), no. 5 052007, [1809.03290].

[7] **BaBar** Collaboration, J. P. Lees *et al. Phys. Rev. Lett.* **123** (2019), no. 9 091801, [1903.10002].

[8] D. Bigi, P. Gambino, and S. Schacht *Phys. Lett.* **B769** (2017) 441–445, [1703.06124].

[9] D. Bigi, P. Gambino, and S. Schacht *JHEP* **11** (2017) 061, [1707.09509].

[10] P. Gambino, M. Jung, and S. Schacht *Phys. Lett.* **B795** (2019) 386–390, [1905.08209].

[11] B. Grinstein and A. Kobach *Phys. Lett.* **B771** (2017) 359–364, [1703.08170].

[12] A. Abdesselam *et al.* 1702.01521.

[13] BELLE. Private communication with Phillip Urquiso, 2019.

[14] https://hflav-eos.web.cern.ch/hflav-eos/semi/spring19/main.shtml.

[15] M. Bordone, M. Jung, and D. van Dyk 1908.09398.

[16] Y. Amhis *et al. Eur. Phys. J.* **C77** (2017), no. 12 895, [1612.07233].

[17] T. Blum *et al. Phys. Rev.* **D91** (2015), no. 7 074502, [1502.00263].

[18] Z. Bai *et al. Phys. Rev. Lett.* **115** (2015), no. 21 212001, [1505.07863].

[19] J. Charles *et al. Eur.Phys.J.* **C41** (2005) 1–131, [hep-ph/0406184]. updated results and plots available at: http://ckmfitter.in2p3.fr.

[20] M. Bona *et al. JHEP* **10** (2006) 081, [hep-ph/0606167]. Standard Model fit results: Summer 2016 (ICHEP 2016): http://www.utfit.org.

[21] M. Tanabashi *et al. Phys. Rev.* **D98** (2018), no. 3 030001. http://pdg.lbl.gov/2019/.

[22] G. Martinelli *et al.* http://www.utfit.org/UTfit/, 2017.

[23] A. J. Buras and D. Guadagnoli *Phys.Rev.* **D78** (2008) 033005, [0805.3887].

[24] J. Brod and M. Gorbahn *Phys.Rev.* **D82** (2010) 094026, [1007.0684].

[25] **Flavour Lattice Averaging Group** Collaboration, S. Aoki *et al.* 1902.08191.

[26] B. J. Choi *et al. Phys. Rev.* **D93** (2016), no. 1 014511, [1509.00592].

[27] T. Blum *et al. Phys. Rev.* **D93** (2016), no. 7 074505, [1411.7017].

[28] J. Laiho and R. S. Van de Water *PoS* **LATTICE2011** (2011) 293, [1112.4861].

[29] S. Durr *et al. Phys. Lett.* **B705** (2011) 477–481, [1106.3230].

[30] A. J. Buras, D. Guadagnoli, and G. Isidori *Phys.Lett.* **B688** (2010) 309–313, [1002.3612].

[31] N. Christ *et al. Phys.Rev.* **D88** (2013), no. 1 014508, [1212.5931].

[32] N. Christ *et al. PoS* **LATTICE2013** (2014) 397, [1402.2577].

[33] J. Brod, M. Gorbahn, and E. Stamou 1911.06822.

[34] B. J. Choi *et al. PoS* **LATTICE2019** (2019) 050.

[35] S. Jwa *et al. PoS* **LATTICE2019** (2019) 056.

[36] T. Bhattacharya *et al. PoS* **LATTICE2018** (2018) 283, [1812.07675].

[37] J. A. Bailey *et al. EPJ Web Conf.* **175** (2018) 13012, [1711.01786].

[38] J. Bailey, Y.-C. Jang, W. Lee, and J. Leem *EPJ Web Conf.* **175** (2018) 14010, [1711.01777].